ResearchGate

See discussions, stats, and author profiles for this publication at: https://www.researchgate.net/publication/225244133

Uncertainty Modeling and Robust Control for Smart Structures

Chapter · December 2010

DOI: 10.1007/978-94-007-0053-6_15

CITATIONS
2

READS
44

3 authors, including:

Georgios Eleftherios Stavroulakis
Technical University of Crete
389 PUBLICATIONS **2,760** CITATIONS

SEE PROFILE

Anastasios D. Pouliezos
Technical University of Crete
62 PUBLICATIONS **599** CITATIONS

SEE PROFILE

Some of the authors of this publication are also working on these related projects:

EGREENSHIP View project

Special Issue "Advances in Architectural Acoustics" – Applied Sciences (MDPI) View project

All content following this page was uploaded by Anastasios D. Pouliezos on 23 May 2014.

The user has requested enhancement of the downloaded file.

Uncertainty Modeling and Robust Control for Smart Structures

A. Moutsopoulou, G.E. Stavroulakis, and A. Pouliezos

Abstract In this work a robust control problem for smart beams is studied. First the structural uncertainties of basic physical parameters are considered in the model of a composite beam with piezoelectric sensors and actuators subjected to wind-type loading. The control mechanism is introduced and is designed with the purpose to keep the bean in equilibrium in the event of external wind disturbances and in the presence of mode inaccuracies using the available measurement and control under limits. For this model we considered the analysis and synthesis of a H_∞-controller with the aim to guarantee the robustness with respect to parametric uncertainties of the beam and of external loads. In addition a robust m-controller was analyzed and synthesized, using the $D - K$ Iterative method. The results are compared and commented upon using the various controllers.

Keywords Uncertainty · Smart beam · Stochastic load · Robust performance · Robust analysis · Robust synthesis

1 Introduction

The field of smart structures has been an emerging area of research for the last few decades [2–5, 9]. Smart structures (also called smart material structures) can be defined as structures that are capable of sensing and actuating in a controlled manner in response to a stimulus. The development of this field is supported by the development in the field of materials science and in the field of control. In materials science, new smart materials are developed that allow them to be used for sensing and actuation in an efficient and controlled manner. These smart materials are to be integrated with the structures so they can be employed as actuators and sensors

A. Moutsopoulou, G.E. Stavroulakis (✉), and A. Pouliezos
Department of Production Engineering and Management, Technical University of Crete, GR-73100 Chania, Greece
e-mail: amalia@dpem.tuc.gr; gestavr@dpem.tuc.gr; tasos@dpem.tuc.gr

M. Papadrakakis et al. (eds.), *Computational Methods in Earthquake Engineering*, Computational Methods in Applied Sciences 21, DOI 10.1007/978-94-007-0053-6_15,
© Springer Science+Business Media B.V. 2011

effectively. It is also clear that the field of smart structures also involves the design and implementation of the control systems on the structures. A well designed and implemented controller for smart structures is thus desirable.

In this paper we introduce uncertainties in smart structures. The control system aims at suppressing undesirable ones and/or enhancing desirable effects. We study an example of such a structure: an intelligent beam with integrated piezoelectric actuators, the goal of which is to suppress oscillations under stochastic loads. First we examine the H_∞ criterion which takes into account the worst case scenarion of uncertain disturbances or noise in the system. Therefore, it is possible to synthesize a H_∞ controller which will be robust with respect to a predefined number of uncertainties in the model. Then by which among other, may take into account non-linearity of the structure, damage or other changes from the nominal model, a robust m-controller was analyzed and synthesized, using the $D-K$ iterative method. The results are very good: the oscillations were suppressed even for a real aeolian load, with the voltages of the piezoelectric components' lying within their endurance limits.

2 Mathematical Modelling

A cantilever slender beam with rectangular cross-sections is considered. Four pairs of piezoelectric patches are embedded symmetrically at the top and the bottom surfaces of the beam, as shown in Fig. 1. The beam is from graphite-epoxy $T300-976$ and the piezoelectric patches are $PZTG1195N$. The top patches act like sensors and the bottom like actuators. The resulting composite beam is modelled by means of the classical laminated technical theory of bending. Let us assume that the mechanical

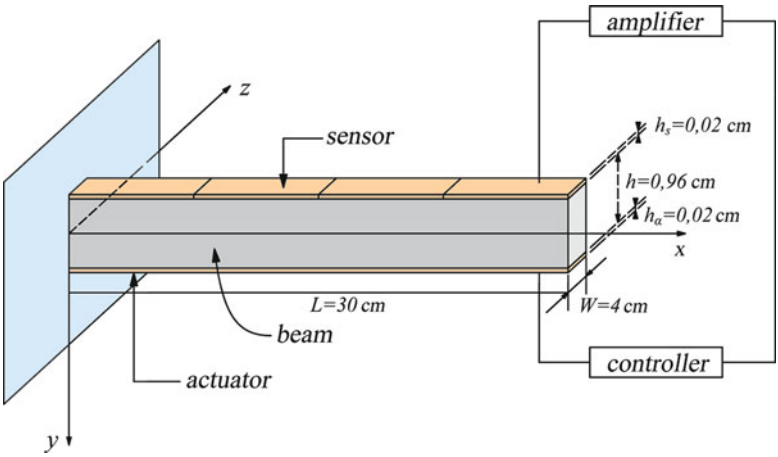

Fig. 1 Beam with piezoelectric sensors/actuators

properties of both the piezoelectric material and the host beam are independent in time. The thermal effects are considered to be negligible as well [9].

The beam has length L, width b and thickness h. The sensors and the actuators have width b_S and b_A and thickness h_S and h_A, respectively. The electromechanical parameters of the beam of interest are given in the table.

Parameters of the Composite Beam

Parameters	Values
Beam length, L	0.3 m
Beam width, W	0.04 m
Beam thickness, h	0.0096 m
Beam density, ρ	1600 kg/m
Youngs modulus of the beam, E	1.5×10^{11} N/m^2
Piezoelectric constant, d_{31}	254×10^{-12} m/V
Electric constant, ξ_{33}	11.5×10^{-3} Vm/N
Young's modulus of the piezoelectric element	1.5×10^{11} N/m^2
Width of the piezoelectric element	$b_S = b_a = 0.04$ m
Thickness of the piezoelectric element	$h_S = h_a = 0.0002$ m

2.1 Piezoelectric Equations

In order to derive the basic equations for piezoelectric sensors and actuators (S/As), we assume that:

- The piezoelectric S/A are bonded perfectly on the host beam;
- The piezoelectric layers are much thinner then the host beam;
- The piezoelectric material is homogeneous, transversely isotropic and linearly elastic;
- The piezoelectric S/A are transversely polarized (in the z-direction) [9].

Under these assumptions the three-dimensional linear constitutive equations are given by [8],

$$\begin{Bmatrix} \sigma_{xx} \\ \sigma_{xz} \end{Bmatrix} = \begin{bmatrix} Q_{11} & 0 \\ 0 & Q_{55} \end{bmatrix} \left(\begin{Bmatrix} \varepsilon_{xx} \\ \varepsilon_{xz} \end{Bmatrix} - \begin{bmatrix} d_{31} \\ 0 \end{bmatrix} E_z \right) \tag{1}$$

$$D_z = Q_{11} d_{31} \varepsilon_{xx} + \xi_{xx} E_z \tag{2}$$

where σ_{xx}, σ_{xz} denote the axial and shear stress components, D_z, denotes the transverse electrical displacement; ε_{xx} and ε_{xz} are a axial and shear strain components; Q_{11}, and Q_{55}, denote elastic constants; d_{31}, and ξ_{33}, denote piezoelectric and dielectric constants, respectively. Equation (1) describes the inverse piezoelectric effect and Eq. (2) describes the direct piezoelectric effect. E_z, is the transverse

component of the electric field that is assumed to be constant for the piezoelectric layers and its components in the xy-plain are supposed to vanish. If no electric field is applied in the sensor layer, the direct piezoelectric Eq. (2) gets the form,

$$D_z = Q_{11} d_{31} \varepsilon_{xx} \tag{3}$$

and it is used to calculate the output charge created by the strains in the beam [7].

2.2 Equations of Motion

We assume that:

- The beam centroidal and elastic axis coincides with the x-coordinate axis so that no bending-torsion coupling is considered;
- The axial vibration of the host beam is considered negligible;
- The displacement field $\{u\} = (u_1, u_2, u_3)$ is obtained based on the usual Timoshenko assumptions [1],

$$\begin{aligned} u_1(x, y, z) &\approx z\phi(x, t) \\ u_2(x, y, z) &\approx 0 \\ u_3(x, y, x) &\approx w(x, t) \end{aligned} \tag{4}$$

where ϕ is the rotation of the beam's cross-section about the positive y-axis and w is the transverse displacement of a point of the centroidal axis ($y = z = 0$).

The strain displacement relations can be applied to Eq. (4) to give,

$$\varepsilon_{xx} = z\frac{\vartheta \phi}{\vartheta x} \quad \varepsilon_{xz} = \phi + \frac{\vartheta w}{\vartheta x} \tag{5}$$

We suppose that the transverse shear deformation ε_{xx} is equal to zero [2].

In order to derive the equations of the motion of the beam we use Hamilton's principle,

$$\int_{t_2}^{t_1} (\delta T - \delta U + \delta W) dt = 0, \tag{6}$$

where T [11] is the total kinetic energy of the system, U is the potential (strain) energy and W is the virtual work done by the external mechanical and electrical loads and moments. The first variation of the kinetic energy is given by,

$$\begin{aligned} \delta T &= \frac{1}{2} \int_V \rho \left\{ \frac{\vartheta u}{\vartheta t} \right\}^r \left\{ \frac{\vartheta u}{\vartheta t} \right\} dV \\ &= \frac{b}{2} \int_0^L \int_{-\frac{h}{2}-h_a}^{\frac{h}{2}+h_s} \rho \left(z\frac{\vartheta \phi}{\vartheta t} \delta \frac{\vartheta \phi}{\vartheta t} + \frac{\vartheta w}{\vartheta t} \delta \frac{\vartheta w}{\vartheta t} \right) dz dx \end{aligned} \tag{7}$$

The first variation of the kinetic energy is given by,

$$\begin{aligned}\delta U &= \frac{1}{2}\int_V \delta\{\epsilon\}^T\{\sigma\}dV \\ &= \frac{b}{2}\int_0^L \int_{-\frac{h}{2}-h_a}^{\frac{h}{2}+h_s}\left[Q_{11}\left(z\frac{\vartheta w}{\vartheta x}\delta\right)\left(z\frac{\vartheta w}{\vartheta x}\right)\right]dzdx\end{aligned} \tag{8}$$

If the load consists only of moments induced by piezoelectric actuators and since the structure has no bending twisting couple then the first variation of the work has the form [11],

$$\delta W = b\int_0^L M^a\delta\left(\frac{\vartheta\phi}{\vartheta x}\right)dx \tag{9}$$

where M^a is the moment per unit length induced by the actuator layer and is given by,

$$M^a = \int_{-\frac{h}{2}-h_a}^{-\frac{h}{2}} z\sigma_{xx}^a dz = \int_{-\frac{h}{2}-h_a}^{-\frac{h}{2}} zQ_{11}d_{31}E_z^a dz\left(E_z^a = \frac{V_a}{h_a}\right) \tag{10}$$

2.3 Finite Element Formulation

We consider a beam element of length L_e, which has two mechanical degrees of freedom at each node: one translational ω_1 (respectively ω_2) in direction y and one rotational ψ_1 (respectively ψ_2), as it is shown in Fig. 2.

The vector of nodal displacements and rotations q_e is defined as [8],

$$q_e = [\omega_1, \psi_1, \omega_2, \psi_2] \tag{11}$$

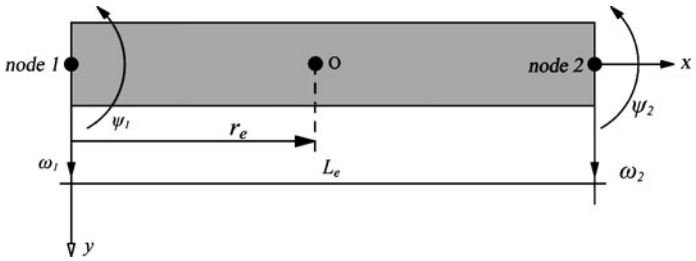

Fig. 2 Beam finite element

The transverse deflection $\omega(x,t)$ and rotation $\psi(x,t)$ along the beam are continuous and they are interpolated by Lagrange linear shape functions H_i^{ω} and H_i^{ψ} as follows [5],

$$\omega(x,t) = \sum_{i=1}^{4} H_i^{\omega}(x) q_i(t)$$
$$\psi(x,t) = \sum_{i=1}^{4} H_i^{\psi}(x) q_i(t) \tag{12}$$

This classical finite element procedure leads to the approximate (discretized) problem. For a finite element the discrete differential equations are obtained by substituting the discretized expressions (12) into Eqs. (7) and (8) to evaluate the kinetic and strain energies. Integrating over spatial domains and using the Hamilton's principle (6) the equation of motion for a beam element are expressed in terms of nodal variable q as follows [2,6,8],

$$M\ddot{q}(t) + D\dot{q}(t) + Kq(t) = f_m(t) + f_e(t) \tag{13}$$

where M is the generalized mass matrix, D the viscous damping matrix, K the generalized stiffness matrix, f_m the external loading vector and f_e the generalized control force vector produced by electromechanical coupling effects. The independent variable vector $q(t)$ is composed of transversal deflections ω_i and rotations ψ_i, i.e., [4]

$$q(t) = \begin{bmatrix} \omega_1 \\ \psi_1 \\ \vdots \\ \omega_n \\ \psi_n \end{bmatrix} \tag{14}$$

where n is the number of nodes used in the analysis. Vectors w and f_m are positive upwards. For the state-space control transformation, let (in the usual manner),

$$\dot{x}(t) = \begin{bmatrix} q(t) \\ \dot{q}(t) \end{bmatrix} \tag{15}$$

Furthermore to express $f_e(t)$ as $Bu(t)$ we write it as $f_e^* u$, where f_e^* is the piezoelectric force for a unit applied on the corresponding actuator, and u represents the voltages on the actuators. Furthermore, $d(t) = f_m(t)$ is the disturbance vector [3]. Then,

$$\dot{x}(t) = \begin{bmatrix} 0_{2n\times 2n} & I_{2n\times 2n} \\ -M^{-1}K & -M^{-1}D \end{bmatrix} x(t) + \begin{bmatrix} 0_{2n\times n} \\ M^{-1} f_e^* \end{bmatrix} u(t) + \begin{bmatrix} 0_{2n\times 2n} \\ M^{-1} \end{bmatrix} \tag{16}$$

$$= Ax(t) + Bu(t) + Gd(t) = Ax(t) + \begin{bmatrix} B & G \end{bmatrix} \begin{bmatrix} u(t) \\ d(t) \end{bmatrix} = Ax(t) + \tilde{B}\tilde{u}(t) \quad (17)$$

The previous description of the dynamical system will be augmented with the output equation (*displacements* only measured) [5],

$$y(t) = [x_1(t) \quad x_3(t) \quad \dots \quad x_{n-1}(t)]^T = Cx(t) \quad (18)$$

In this formulation u is $n \times 1$ (at most, but can be smaller), while d is $2n \times 1$. The units used are compatible for instance m, rad, sec and N [6, 8].

3 Design Objectives and System Specifications

The structured singular value of the transfer function is defined as,

$$\mu(M) = \begin{cases} \frac{1}{\min_{k_m}\{det(I - k_m M\Delta) = 0,\ \bar{\sigma}(\Delta) \leq 1\}} \\ 0, \ \Delta \ det(I - M\Delta) = 0 \end{cases} \quad (19)$$

In words it defines the smallest structured $\mu(M)$ (measured in terms of $\bar{\sigma}(\Delta)$) which makes $det(I - M\Delta) = 0$: then $\mu(M) = \frac{1}{\bar{\sigma}(\Delta)}$. It follows that values of μ smaller than 1 are desired [12].

The design objectives fall into two categories:

1. Stability of closed loop system (plant+controller).
   a. Disturbance attenuation with satisfactory transient characteristics (overshoot, settling time).
   b. Small control effort.
2. Robust performance

Stability of closed loop system (plant+controller) should be satisfied in the face of modelling errors.

In order to obtain the required system specifications with respect to the above objectives we need to represent our system in the so-called - Δ structure. Let us start with the simple typical diagram of Fig. 3 [13, 14].

In this diagram there are two inputs, d and n, and two outputs, u and x. In what follows it is assumed that,

$$\left\| \begin{matrix} d \\ n \end{matrix} \right\|_2 \leq 1, \quad \left\| \begin{matrix} x \\ u \end{matrix} \right\|_2 \leq 1 \quad (20)$$

If that's not the case, appropriate frequency-dependent weights can transform original signals so that the transformed signals have this property. The details of the system are given in Fig. 4.

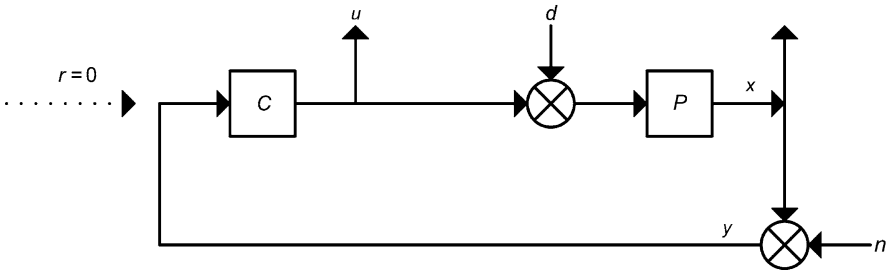

Fig. 3 Classical control block diagram (P: plant dynamical system, C: controller)

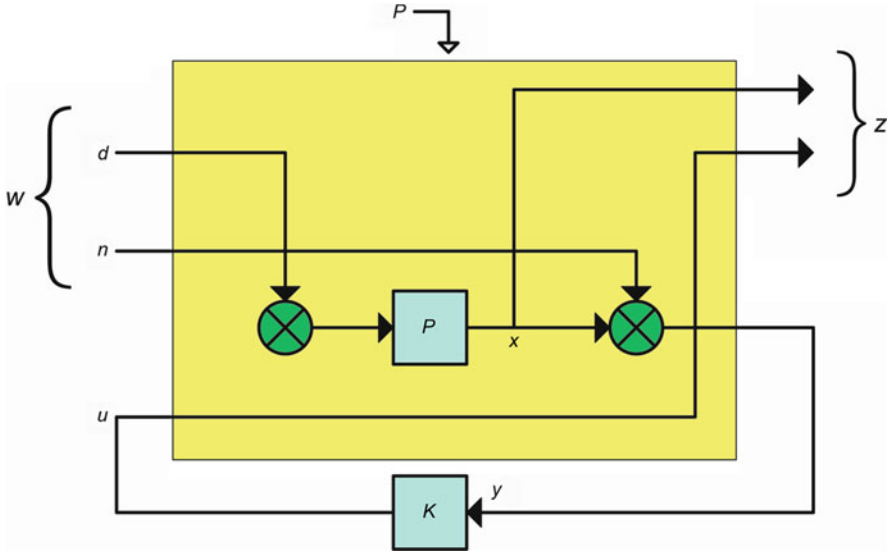

Fig. 4 Detailed two-port diagram (with a linear feedback control K)

In this description,

$$z = \begin{bmatrix} u \\ x \end{bmatrix}, \quad w = \begin{bmatrix} d \\ n \end{bmatrix} \tag{21}$$

where z are the output variables to be controlled, and w the exogenous inputs.

Given that P has two inputs and two outputs it is (Fig. 5), as usual, naturally partitioned as,

$$\begin{bmatrix} z(s) \\ y(s) \end{bmatrix} = \begin{bmatrix} P_{zw}(s) & P_{zu}(s) \\ P_{yw}(s) & P_{yu}(s) \end{bmatrix} \begin{bmatrix} w(s) \\ u(s) \end{bmatrix} = P(s) \begin{bmatrix} w(s) \\ u(s) \end{bmatrix} \tag{22}$$

In addition the controller is written,

$$u(s) = K(s)y(s) \tag{23}$$

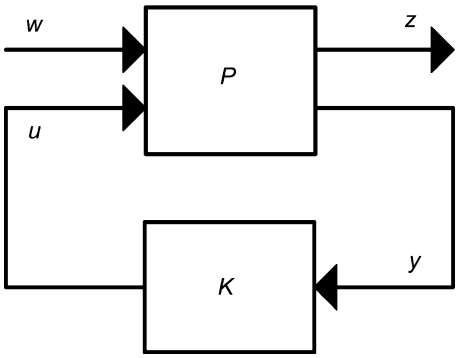

Fig. 5 Two-port diagram

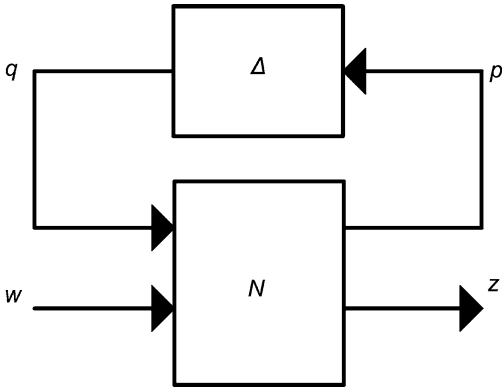

Fig. 6 Two-port diagram with uncertainty

Substituting Eq. (22) in Eq. (23) gives the closed loop transfer function $N_{zw}(s)$,

$$N_{zw}(s) = P_{zw}(s) + P_{zu}(s)K(s)(I - P_{yu}(s)K(s))^{-1}P_{yw}(s) \tag{24}$$

To deduce robustness specifications a further diagram is needed, namely that of Fig. 6: where N is defined by Eq. (24) and the uncertainty modelled in Δ satisfies $||\Delta||_\infty \leq 1$ (details later). Here,

$$z = \mathscr{F}_u(N, \Delta)w = [N_{22} + N_{21}\Delta(I - N_{11}\Delta)^{-1}N_{12}]w = Fw \tag{25}$$

Given this structure we can state the following definitions:

$$\begin{gathered}
\text{Nominal stability } (NS) \Leftrightarrow N \text{ internally stable} \\
\text{Nominal performance } (NP) \Leftrightarrow ||N_{22}(j\omega)||_\infty \leq 1 \ \forall\omega \text{ and } NS \\
\text{Robust stability } (RS) \Leftrightarrow F = \mathscr{F}_u(N, \Delta) \text{ stable } \forall\Delta,\ ||\Delta||_\infty < 1 \text{ and } NS \\
\text{Robust performance } (RP) \Leftrightarrow ||F||_\infty < 1,\ \forall\Delta,\ ||\Delta||_\infty < 1 \text{ and } S
\end{gathered} \tag{26}$$

It has been proved that the following conditions hold in the case of block-diagonal real or complex perturbations Δ:

1. The system is nominally stable if M is internally stable.
2. The system exhibits nominal performance if $\bar{\sigma}(N_{22}(j\omega)) < 1$.
3. The system (M, Δ) is robustly stable if and only if,

$$\sup_{\omega \in \mathbb{R}} \mu_{\Delta}(N_{11}(j\omega)) < 1 \tag{27}$$

   where μ_{Δ} is the structured singular value of N given the structured uncertainty set Δ. This condition is known as the generalized small gain theorem.
4. The system (N, Δ) exhibits robust performance if and only if,

$$\sup_{\omega \in \mathbb{R}} \mu_{\Delta_a}(N(j\omega)) < 1 \tag{28}$$

   where,

$$\Delta_a = \begin{bmatrix} \Delta_p & 0 \\ 0 & \Delta \end{bmatrix} \tag{29}$$

   and Δ_p is full complex, has the same structure as Δ and dimensions corresponding to w, z [15].
   Unfortunately, only bounds on μ can be estimated.

3.1 Controller Synthesis

All the above results support the analysis problem and provide tools to judge the performance of any controller or to compare different controllers. However it is possible to approximately synthesize a controller that achieves given performance in terms of the structured singular value μ.

In this procedure, which is called $(D, G - K)$ iteration [20] the problem of finding an μ-optimal controller K such that $\mu(\mathscr{F}_u(F(j\omega)), K(j\omega)) \leq \beta$, $\forall \omega$ is transformed into the problem of finding transfer function matrices $D(\omega) \in \mathscr{D}$ and $G(\omega) \in \mathscr{G}$, such that,

$$\sup_{\omega} \bar{\sigma} \left[\left(\frac{D(\omega)\mathscr{F}_u(F(j\omega), K(j\omega))D^{-1}(\omega)}{\gamma} - jG(\omega) \right) \left(I + G^2(\omega)\right)^{-\frac{1}{2}} \right] \leq 1, \quad \forall \omega \tag{30}$$

Unfortunately this method does not guarantee even finding local maxima. However for complex perturbations a method known as $D-K$ iteration is available (implemented in MATLAB) [20]. It combines H_{∞} synthesis and μ-analysis and often yields good results. The starting point is an upper bound on μ in terms of the scaled singular value,

$$\mu(N) \leq \min_{D \in \mathscr{D}} \bar{\sigma}(DND^{-1}) \tag{31}$$

The idea is to find the controller that minimizes the peak over the frequency range namely,

$$\min_{K}\left(\min_{D\in\mathscr{D}}||DN(K)D^{-1}||_{\infty}\right) \tag{32}$$

by alternating between minimizing $||DN(|K)D^{-1}||_{\infty}$ with respect to either K or D (while holding the other fixed).

1. **K-step**. Synthesize an $\mathscr{H}_{\infty}$ controller for the scaled problem $\min_K ||DN(K)$ $D^{-1}||_{\infty}$ with fixed $D(s)$.
2. **D-step**. Find $D(j\omega)$ to minimize at each frequency $\bar{\sigma}(DND^{-1}(j\omega))$ with fixed N.
3. Fit the magnitude of each element of $D(j\omega)$ to a stable and minimum phase transfer function $D(s)$ and got to Step 1 [20].

3.2 System Uncertainty

Let us assume uncertainty in the mass M and K matrices of the form,

$$\begin{aligned} K &= K_0(I + k_p I_{2n\times 2n}\delta_K) \\ M &= M_0(I + m_p I_{2n\times 2n}\delta_M) \end{aligned} \tag{33}$$

Alternatively, since in general the Rayleigh damping assumption is,

$$D = aK + \beta M \tag{34}$$

D could be expressed similarly to K, M, as,

$$D = D_0(I + d_p I_{2n\times 2n}\delta_D) \tag{35}$$

In this way we introduce uncertainty in the form of percentage variation in the relevant matrices. Uncertainty is most likely to arise from terms outside the main matrices (since length can be adequately measured).

Here it will be assumed,

$$||\Delta||_{\infty} \stackrel{def}{=} \left\| \left[\begin{array}{c|c} I_{n\times n}\delta_K & 0_{n\times n} \\ \hline 0_{n\times n} & I_{n\times n}\delta_M \end{array}\right] \right\|_{\infty} < 1 \tag{36}$$

hence m_p, k_p are used to scale the percentage value and the zero subscript denotes nominal values. (it is reminded that the norm for a matrix $A_{n\times n}$ is calculated through $||A||_{\infty} = \max_{1\le j\le m}\sum_{j=1}^{n}|a_{ij}|$)

With these definitions Eq. 13 becomes,

$$
\begin{aligned}
&M_0(I + m_p I_{2n\times 2n}\delta_M)\ddot{w}(t) + K_0(I + k_p I_{2n\times 2n}\delta_K)w(t) \\
&\quad + [D_0 + 0.0005[K_0 k_p I_{2n\times 2n}\delta_K + M_0 m_p I_{2n\times 2n}\delta_M]]\dot{w}(t) \\
&= f_m(t) + f_e(t) \\
&\Rightarrow M_0\ddot{w}(t) + D_0\dot{q}(t) + K_0 w(t) = -[M_0 m_p I_{2n\times 2n}\delta_M \ddot{w}(t) \\
&\quad + 0.0005[K_0 k_p I_{2n\times 2n}\delta_K + M_0 m_p I_{2n\times 2n}\delta_M]\dot{w}(t) + K_0 k_p I_{2n\times 2n}\delta_K w(t)] \\
&= f_m(t) + f_e(t) \\
&\Rightarrow M_0\ddot{w}(t) + D_0\dot{w}(t) + K_0 w(t) = \tilde{D}q_u(t) + f_m(t) + f_e(t)
\end{aligned} \tag{37}
$$

where,

$$
q_u(t) = \begin{bmatrix} \ddot{w}(t) \\ \dot{w}(t) \\ w(t) \end{bmatrix} \tag{38}
$$

$$
\begin{aligned}
\tilde{D} &= -\begin{bmatrix} M_0 m_p & K_0 k_p \end{bmatrix} \left[\begin{array}{c|c} I_{2n\times 2n}\delta_M & 0_{2n\times 2n} \\ \hline 0_{2n\times 2n} & I_{2n\times 2n}\delta_K \end{array}\right] \begin{bmatrix} I_{2n\times 2n} & 0.0005 I_{2n\times 2n} & 0_{2n\times 2n} \\ 0_{2n\times 2n} & 0.0005 I_{2n\times 2n} & I_{2n\times 2n} \end{bmatrix} \\
&= G_1 \cdot \Delta \cdot G_2
\end{aligned} \tag{39}
$$

Writing (37) in state space form, gives,

$$
\begin{aligned}
\dot{x}(t) &= \begin{bmatrix} 0_{2n\times 2n} & I_{2n\times 2n} \\ -M^{-1}K & -M^{-1}D \end{bmatrix} x(t) + \begin{bmatrix} 0_{2n\times 2n} \\ M^{-1} f_e^* \end{bmatrix} u(t) + \begin{bmatrix} 0_{2n\times 2n} \\ M^{-1} \end{bmatrix} d(t) \\
&\quad + \begin{bmatrix} 0_{2n\times 6n} \\ M^{-1}F_1 \cdot \Delta \cdot G_2 \end{bmatrix} q_u(t) \\
&= Ax(t) + Bu(t) + Gd(t) + G_u G_2 q_u(t)
\end{aligned} \tag{40}
$$

In this way we treat uncertainty in the original matrices as an extra uncertainty term. To express our system in the form of Fig. 6, consider Fig. 7.

The matrices E_1, E_2 are used to extract,

$$
q_u(t) \overset{def}{=} \begin{bmatrix} \ddot{w}(t) \\ \dot{w}(t) \\ w(t) \end{bmatrix} \tag{41}
$$

Since,

$$
\gamma = \begin{bmatrix} \dot{w}(t) \\ \ddot{w}(t) \end{bmatrix} \qquad \beta = \int \begin{bmatrix} \dot{w}(t) \\ \ddot{w}(t) \end{bmatrix} dt = \begin{bmatrix} w(t) \\ \dot{w}(t) \end{bmatrix} \tag{42}
$$

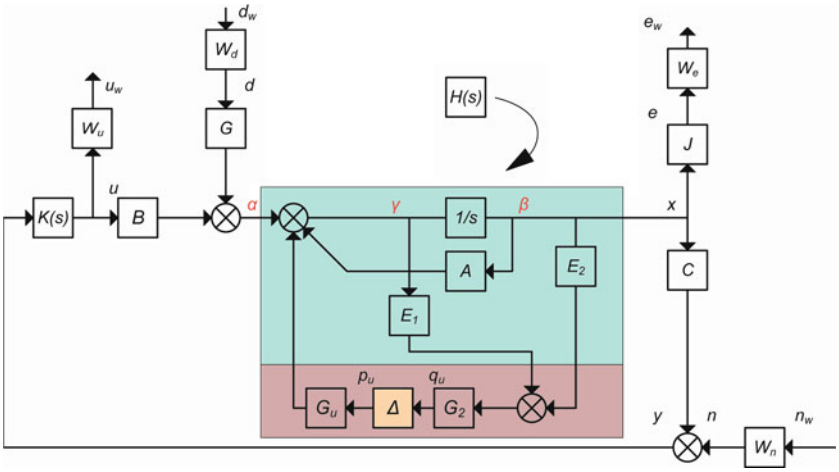

Fig. 7 Uncertainty block diagram

appropriate choices for E_1, E_2 are,

$$E_1 = \begin{bmatrix} 0_{2n\times 2n} & \vdots & I_{2n\times 2n} \\ \cdots & \vdots & \cdots \\ I_{2n\times 2n} & \vdots & 0_{2n\times 2n} \\ \cdots & \vdots & \cdots \\ 0_{2n\times 2n} & \vdots & 0_{2n\times 2n} \end{bmatrix}, \quad E_2 = \begin{bmatrix} 0_{2n\times 2n} & \vdots & 0_{2n\times 2n} \\ \cdots & \vdots & \cdots \\ 0_{2n\times 2n} & \vdots & 0_{2n\times 2n} \\ \cdots & \vdots & \cdots \\ I_{2n\times 2n} & \vdots & 0_{2n\times 2n} \end{bmatrix} \tag{43}$$

The idea is to find an N such that,

$$\begin{bmatrix} q_u \\ \cdots \\ e_w \\ u_w \end{bmatrix} = N \begin{bmatrix} p_u \\ \cdots \\ d_w \\ n_w \end{bmatrix}, \quad N = \begin{bmatrix} N_{p_u q_u} & \vdots & N_{d_w q_u} & N_{n_w q_u} \\ \cdots & \vdots & \cdots & \cdots \\ N_{p_u e_w} & \vdots & N_{d_w e_w} & N_{n_w e_w} \\ N_{p_u u_w} & \vdots & N_{d_w u_w} & N_{n_w u_w} \end{bmatrix} = \begin{bmatrix} N_{11} & N_{12} \\ N_{21} & N_{22} \end{bmatrix} \tag{44}$$

or in the notation of Fig. 6

$$\begin{bmatrix} q_u \\ w \end{bmatrix} = N \begin{bmatrix} p_u \\ z \end{bmatrix} \tag{45}$$

Now $N_{d_w e_w}$, $N_{n_w e_w}$, $N_{n_w u_w}$ are known. For the rest we will use a methodology known as "pulling out the Δ's". To this end, break the loop at points p_u, q_u (which

will be used as additional inputs/outputs respectively) and use the auxiliary signals a, β, γ. To get the transfer function $N_{d_w q_u}$ (from d_w to q_u):

$$q_u = G_2(E_2\beta + E_1\gamma) = G_2\left(E_2\frac{1}{s} + E_1\right)\gamma \tag{46}$$

$$\gamma = GW_d d_w + Bu + A\frac{1}{s}\gamma = GW_d d_w + BKC\frac{1}{s}\gamma + A\frac{1}{s}\gamma \tag{47}$$

$$\Rightarrow \gamma = \left(I - BKC\frac{1}{s} - A\frac{1}{s}\right)^{-1} GW_d d_w \tag{48}$$

Hence,

$$N_{d_w q_u} = G_2\left(E_2\frac{1}{s} + E_1\right)\left(I - BKC\frac{1}{s} - A\frac{1}{s}\right)^{-1} GW_d \tag{49}$$

Now, $N_{p_u q_u}$, $N_{p_u e_w}$, $N_{p_u u_w}$, are similar to $N_{d_w q_u}$, $N_{d_w e_w}$, $N_{d_w u_w}$, with GW_d replaced by G_u, i.e.,

$$\begin{aligned} N_{p_u q_u} &= G_2\left(E_2\frac{1}{s} + E_1\right)\left(I - BKC\frac{1}{s} - A\frac{1}{s}\right)^{-1} G_u \\ N_{p_u e_w} &= W_y JH[I + B[K(I - CHBK)^{-1}CH]]G_u \\ M_{p_u u_w} &= W_u K(I - CHBK)^{-1}CHG_u \end{aligned} \tag{50}$$

Finally to find $N_{n_w q_u}$,

$$q_u = G_2(E_2\beta + E_1\gamma) = G_2\left(E_2\frac{1}{s} + E_1\right)\gamma \tag{51}$$

$$\gamma = Bu + A\frac{1}{s}\gamma = BK(W_n n_w + y) + A\frac{1}{s}\gamma = BKW_n n_w + BKC\frac{1}{s}\gamma + A\frac{1}{s}\gamma \tag{52}$$

$$\Rightarrow \gamma = \left(I - BKC\frac{1}{s} - A\frac{1}{s}\right)^{-1} BKW_n n_w \tag{53}$$

Hence,

$$N_{n_w q_u} = G_2\left(E_2\frac{1}{+}E_1\right)\left(I - BKC\frac{1}{s} - A\frac{1}{s}\right)^{-1} BKW_n \tag{54}$$

Collecting all the above yields N:

$$N = \begin{bmatrix} G_2\left(E_2\frac{1}{s}+E_1\right)\left(I-BKC\frac{1}{s}-A\frac{1}{s}\right)^{-1}G_u & G_2\left(E_2\frac{1}{s}+E_1\right)\left(I-BKC\frac{1}{s}-A\frac{1}{s}\right)^{-1}GW_d & G_2\left(E_2\frac{1}{s}+E_1\right)\left(I-BKC\frac{1}{s}-A\frac{1}{s}\right)^{-1}BKW_u \\ W_e JH\left[I+BK(I-CHBK)^{-1}CF\right]G_u & W_e J(I-HBKC)^{-1}HGW_d & W_e J(I-HBKC)^{-1}HBKW_u \\ W_u K(I-CHBK)^{-1}CFG_u & W_u(I-KCHB)^{-1}KCHGW_d & W_u(I-KCHB)^{-1}KW \end{bmatrix} \tag{55}$$

Having obtained N for the beam problem, all proposed controllers $K(s)$ can be compared using the structured singular value relations [18, 19, 21].

4 Robustness Issues

The superiority of H_∞ control lies in its ability to take explicitly into account the worst effect of unknown disturbances and noise in the system. Furthermore, at least in theory, it is possible to synthesize an H_∞ controller that is robust to a prescribed amount of modeling errors. Unfortunately, this last possibility is not implementable in some cases, as it will be subsequently illustrated [16, 17].

In what follows, the robustness to modeling errors of the designed H_∞ controller will be analyzed. Furthermore an attempt to synthesize a μ-controller will be presented, and comparisons between the two will be made.

In all simulations, routines from Matlab's Robust Control Toolbox will be used. In particular:

1. For uncertain elements,
2. To calculate bounds on the structured singular value,
3. To calculate a μ-controller.

Numerical models used in all simulations, are implemented in three ways:

1. Through Eq. (56)

$$\begin{aligned} K &= K_0(I + k_p I_{2n\times 2n}\delta_K) \\ M &= M_0(I + m_p I_{2n\times 2n}\delta_M) \\ D &= D_0 + 0,0005[K_0 k_p I_{2n\times 2n}\delta_K + M_0 m_p I_{2n\times 2n}\delta_M] \end{aligned} \tag{56}$$

   and subsequent evaluation of matrix N for specific values of k_p, m_p.
2. By use of Matlab's "uncertain element object". As explained, this form is needed in the D-K robust synthesis algorithm.
3. By Simulink implementation of Fig. 8.

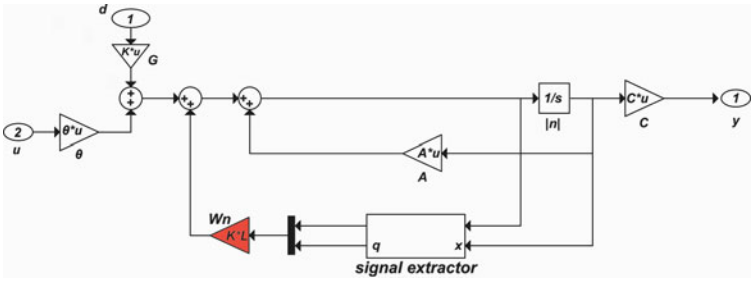

Fig. 8 Simulink diagram of uncertain plant

4.1 Robust Analysis: Results

Robust analysis is carried out through the relations:

$$\sup_{\omega\in\mathbb{R}} \mu_{\Delta}(N_{11}(j\omega)) < 1 \tag{57}$$

for robust stability, and,

$$\sup_{\omega\in\mathbb{R}} \mu_{\Delta_a}(N(j\omega)) < 1 \tag{58}$$

for robust performance.

In all the simulations that follow the disturbance is the first mechanical load, i.e. $10N$ at the free end. For the H_∞ found, robust analysis was performed for the following values of m_p, k_p:

1. $m_p = 0, k_p = 0.9$. This corresponds to a $\pm$ 90% variation from the nominal value of the stiffness matrix K.
   In Fig. 9 are shown the displacement responses for this controller for the first mechanical input. In Fig. 10 are shown the bounds on the μ values. As seen the system remains stable and exhibits robust performance, since the upper bounds of both values remain below 1 for all frequencies of interest. This result is validated in Fig. 11, where the displacement of the free end and the voltage applied are shown at the extreme uncertainty. Comparison with the open loop response for the same plant shows the good performance of the nominal controller.
2. $m_p = 0.9, k_p = 0$. This corresponds to a $\pm$ 90% variation from the nominal value of the mass matrix M.

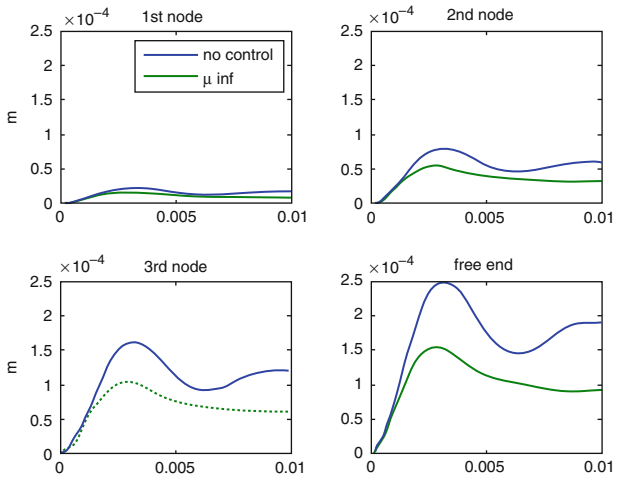

Fig. 9 Displacement response loading equal to 10 N at free end, μ-controller for $m_p = 0, k_p = 0.9$

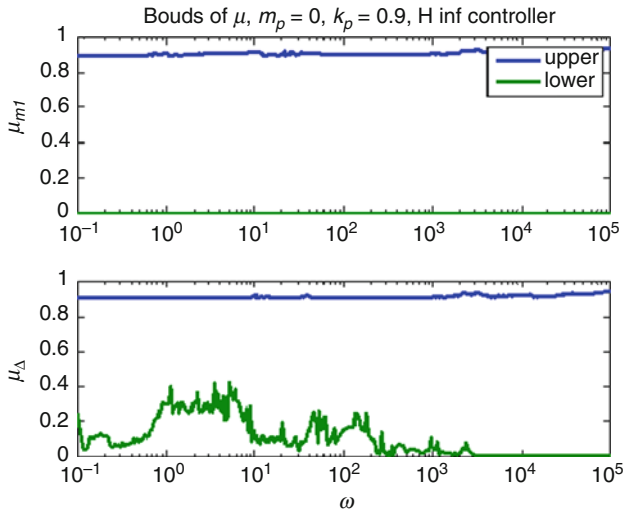

Fig. 10 μ-bounds of the H_∞ controller for $m_p = 0$, $k_p = 0.9$

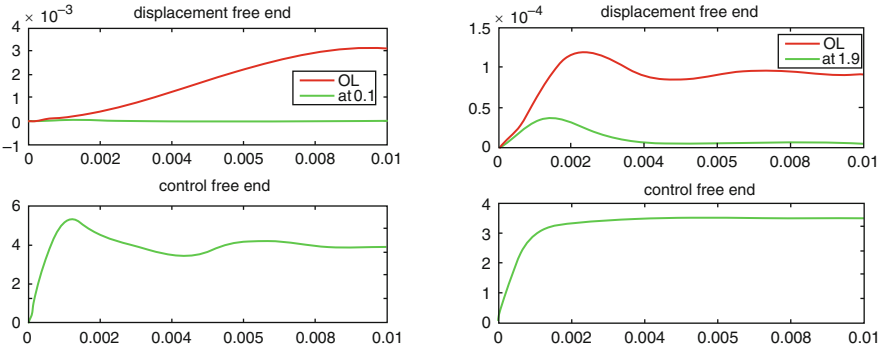

Fig. 11 Displacement and control at free end for the H_∞ controller with $m_p = 0$, $k_p = 0.9$ (extreme values)

In Fig. 12 are shown the bounds on the μ values. As seen the system remains stable and exhibits robust performance, since the upper bounds of both values remain below 1 for all frequencies of interest. This result is validated in Fig. 13, where the displacement of the free end and the voltage applied are shown. Comparison with the open loop response for the same plant shows the good performance of the nominal controller.

3. $m_p = 0.9$, $k_p = 0.9$. This corresponds to a $\pm 90\%$ variation from the nominal values of both the mass and stiffness matrices M, K.

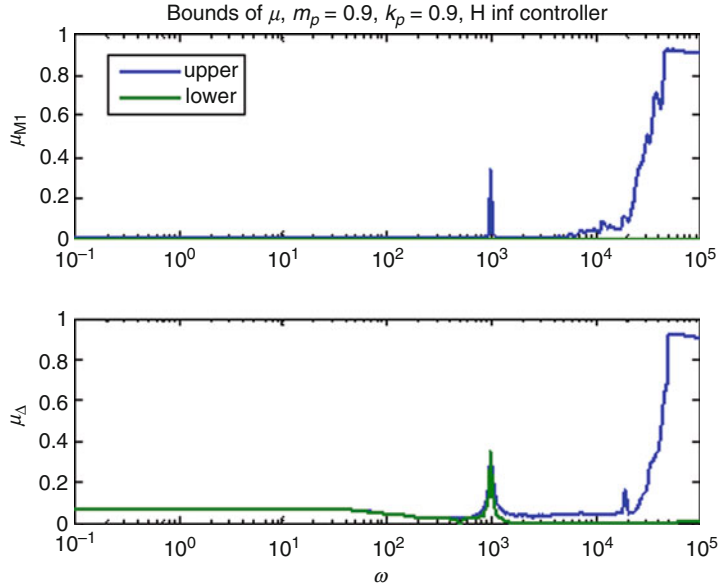

Fig. 12 μ-bounds of the H_∞ controller for $m_p = 0.9$, $k_p = 0$

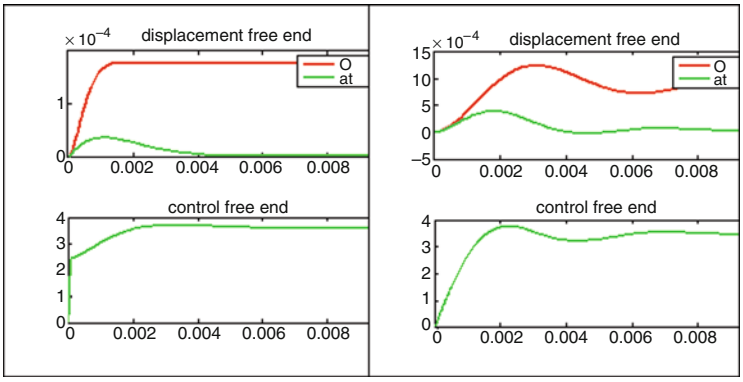

Fig. 13 Displacement and control at free end for the H_∞ controller with $m_p = 0.9$, $k_p = 0$ (extreme values)

In Fig. 14 are shown the bounds on the μ values. As seen the system remains stable and exhibits robust performance, since the upper bounds of both values remain below 1 for all frequencies of interest. This result is validated in Fig. 15, where the displacement of the free end and the voltage applied are shown. Comparison with the open loop response for the same plant shows the good performance of the nominal controller.

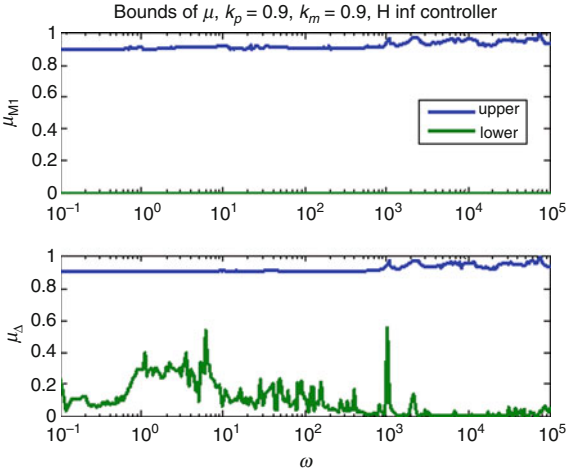

Fig. 14 Displacement and control at free end for the H_∞ controller with $m_p = 0.9$, $k_p = 0$ (extreme values)

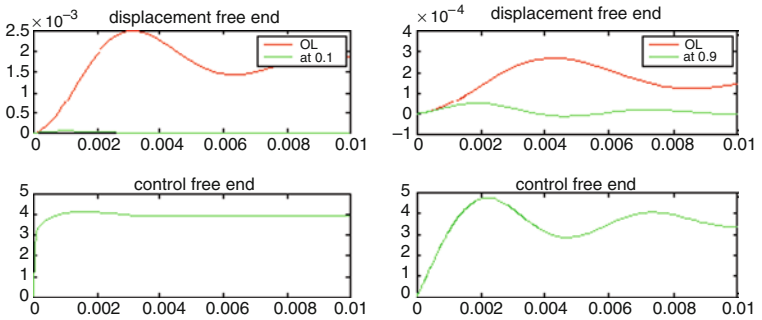

Fig. 15 Displacement and control at free end for the H_∞ controller with $m_p = 0.9$, $k_p = 0$ (extreme values)

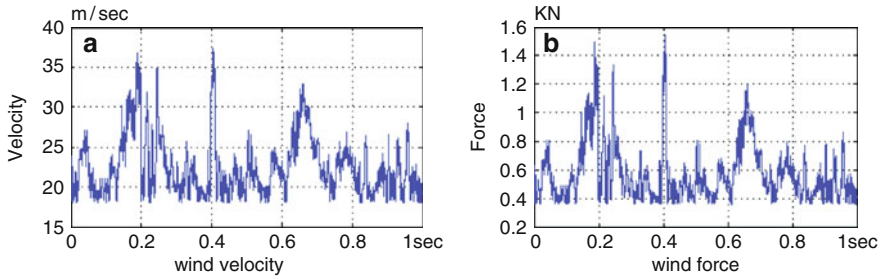

Fig. 16 Wind force and velocity

Concluding, it has been demonstrated that the H_∞ controller found is extremely robust in model variations.

Furthermore, a typical stochastic wind–type load is considered (Fig. 16). We change the mass M, the viscous K and A and B matrices of the system.

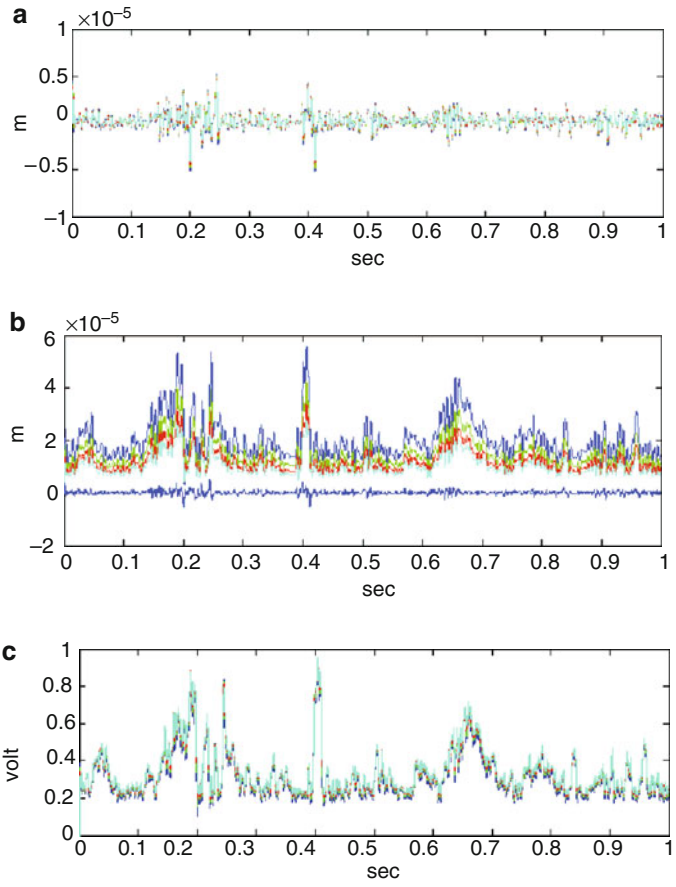

Fig. 17 ± 50% variation from the nominal values of the mass and the viscous matrices (**a**) The displacement of the free end of the beam with control (**b**) The displacement of the free end of the beam with and without control who corresponds to a ± 50% variation from the nominal values of the mass and the viscous matrices (**c**) The applied voltages of the free end

In Fig. 17 are shown the free end of the beam with and without control who corresponds to a ± 50% variation from the nominal value of the mass matrix and the viscous matrix of the beam, and the applied voltages of the free end.

In Fig. 18 are shown the free end of the beam with and without control, who corresponds to a ± 50% variation from the nominal value of the matrix A and B of the beam and the applied voltages of the free end.

The beam with the control keeps in equilibrium and we have zero displacements, event for the changes of the mass, viscous, and the A and B matrices of the system.

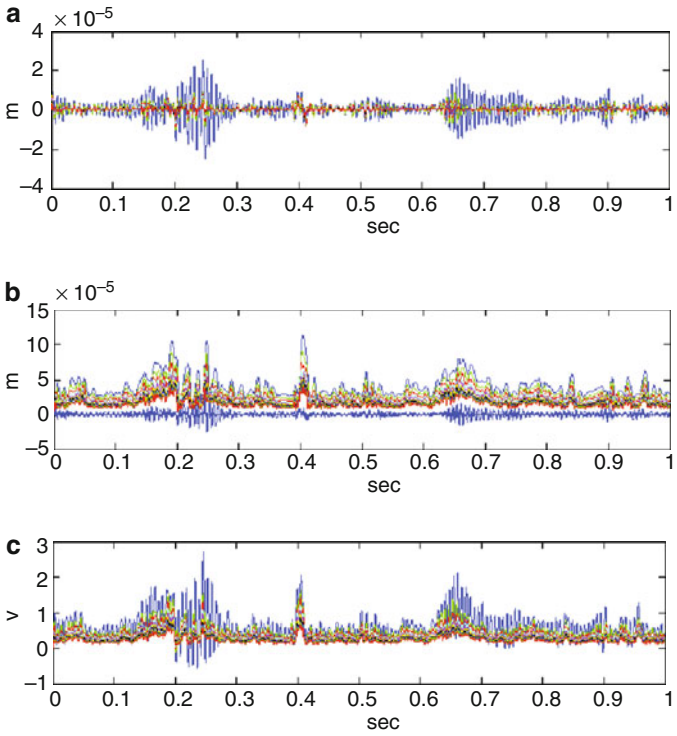

Fig. 18 $\pm$ 50% variation from the nominal values of the A and B (**a**) The displacement of the free end of the beam with control (**b**) The displacement of the free end of the beam with and without control who corresponds to a $\pm$ 50% variation from the nominal values of the matrices A and B of the system (**c**) The applied voltages of the free end

4.2 Robust Synthesis: μ-Controller

A μ-controller can be synthesized via the procedure of D-K μ iteration As explained, this an approximate procedure, providing bounds on the μ-value. To facilitate comparison with the H_∞ controller, similar bounds for the uncertainty will be used.

1. $m_p = 0, k_p = 0.9$. This corresponds to a $\pm 90\%$ variation from the nominal value of the stiffness matrix K.

In Fig. 19 μ-values of the calculated controller are shown. As seen the controller is robust in most frequencies.

In Fig. 20 performance of the μ and H_∞ controllers is compared at the free end (this is indicative of overall performance). As seen the H_∞ controller performs better at the expense of increased control effort. Figure 21 (left window) verifies this result, where it is seen that the H_∞ controller performs better at the extreme value.

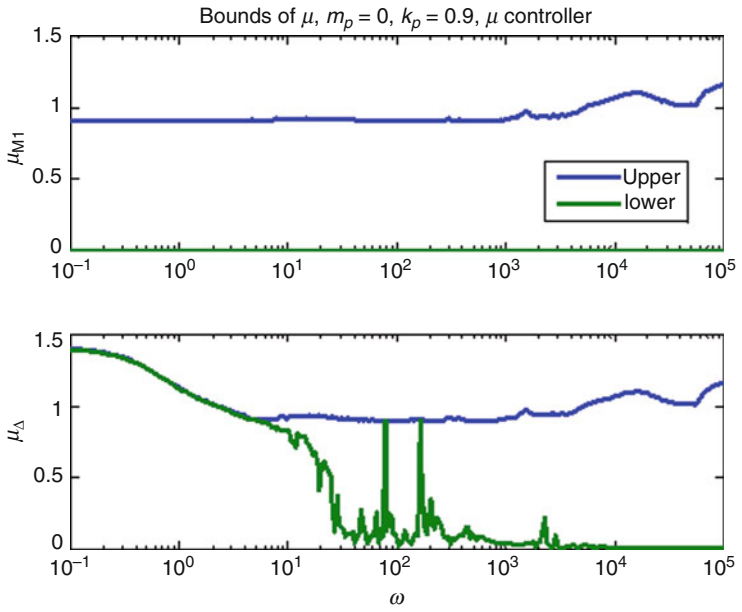

Fig. 19 μ-bounds of the μ-controller for $m_p = 0$, $k_p = 0.9$

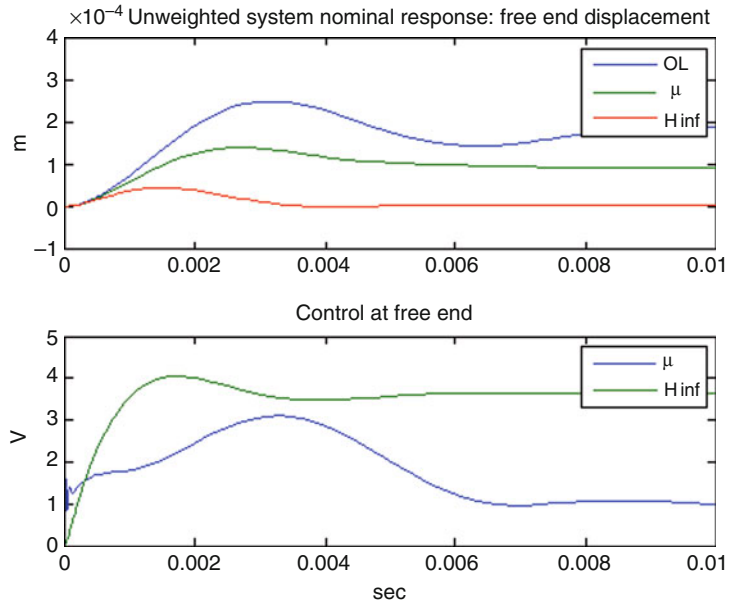

Fig. 20 Comparison of free end data of nominal system for μ-controller ($m_p = 0$, $k_p = 0.9$) and H_∞

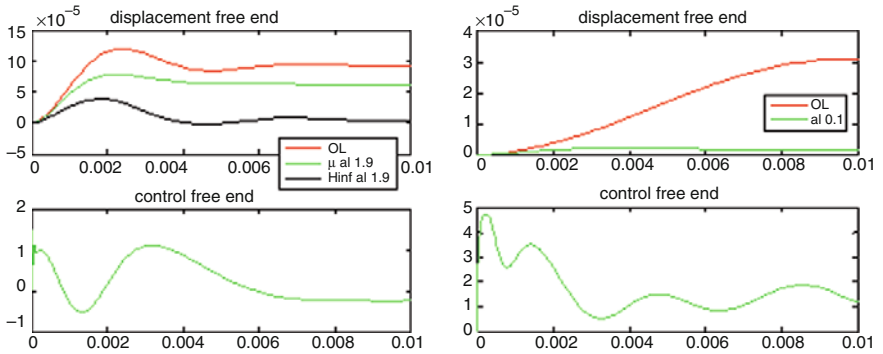

Fig. 21 Displacement and control at free end for the μ-controller with $m_p = 0$, $k_p = 0.9$ (extreme values)

This could be due to numerical difficulties in the calculation of the μ-controller arising from the bad condition number of the plant. It could also be due to the high order of the μ-controller. In any case, further investigation is needed.

5 Reduced Order Control

The H_∞ controller found is of 24th order. Using the Matlab package *HIFOO* we can reduce this controller and stabilize the system with a second order controller without difficulty suggesting explicit formulas for the controller and for the closed loop system.

Furthermore, analytical techniques prove that this controller is locally optimal in the sense that there is no nearby controller with the same order for which the closed loop system has all its poles further left in the complex plane [10, 12].

These approaches can be extended in order to take into account other key quantities of great practical interest, such as optimization of the H_∞ performance. In particular, with the help of a MATLAB toolbox called *HIFOO* (Fixed Order Optimization) we can reduce the order of the controller and have very good results [10].

Figure 22 shows the corresponding control voltages using the 24th order controller for the four nodes of the beam. The beam with H_∞ control keeps in equilibrium and we have zero displacements, as we can see (Fig. 22) the voltage is much lower than 500 V, which is the piezoelectric limit.

Then we use a second order controller for the H_∞ control performance. Figure 23 shows the response of the uncontrolled and controlled beam at the free end, using the second order controller for the stochastic wind load (Fig. 16). Figure 24 shows the corresponding control voltage of the free end. With the help of the controller *HIFOO* we can reduce the order of the system and keep the beam in equilibrium with even lower voltages.

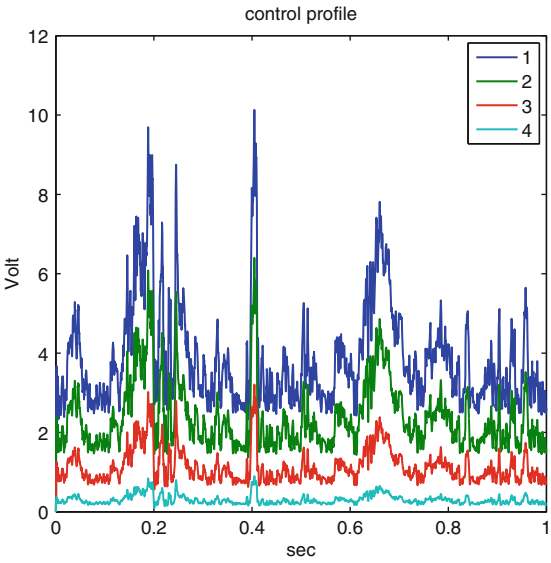

Fig. 22 The control voltages for the four nodes of the beam with the 24th order controller

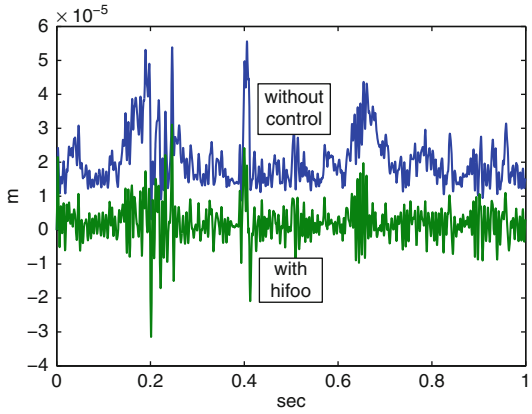

Fig. 23 The displacement of the free end of the beam without and with control with the 2nd order controller

6 Conclusions

A finite element based modelling technique for the determination of the system model of the smart beam was presented. Based on this model an H_∞ and a μ-controller was designed which effectively suppress the vibrations of the smart beam under stochastic wind load.

The advantage of the H_∞ criterion is its ability to take into account the worst influence of uncertain disturbances or noise in the system. It is possible to synthesize a H_∞ controller which will be robust with respect to a prespecified number of errors in the model. Hoping to reduce the model's computational requirements,

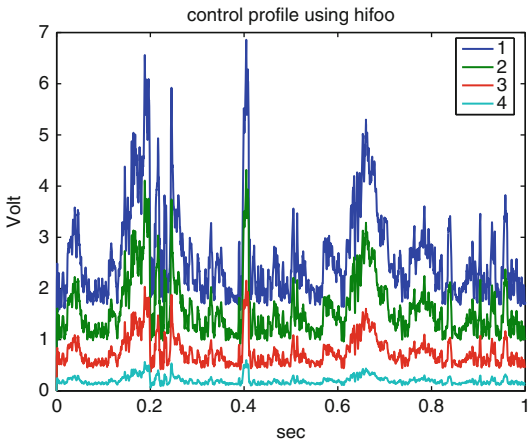

Fig. 24 The control voltages for the four nodes of the beam with the 2nd order controller

the controller's order was reduced, aided by a parametric, nonconvex optimization, and using the *HIFOO* controller. The controller's good performance was maintained even for a much smaller system degree.

Finally taking into account the system's non-linearity which was not considered in the model, our inaccurate knowledge of the model's values and parameters, and their variations over the life of the structure operation, we introduce modeling uncertainties. A robust μ-controller was analyzed and synthesized, using the $D - K$ iterative method. The results are compared and commented upon using the various controllers. The results are very good: the oscillations were suppressed even for a real aeolian load, with the piezoelectric components' voltages within their endurance limits.

References

1. Friedman J, Kosmatka K (1993) An improved two node Timoshenko beam finite element. Comput Struct 47:473–481
2. Foutsitzi G, Marinova D, Hadjigeorgiou E, Stavroulakis G (2003) Robust H2 vibration control of beams with piezoelectric sensors and actuators. Proceedings of physics and control conference (PhyCon03), St. Petersburg, Russia, 20–22 August, vol I, pp 158–163
3. Sisemore C, Smaili A, Houghton R (1999) Passive damping of flexible mechanism system: experimental and finite element investigation. The 10th world congress of the theory of machines and mechanisms, Oulu, Finland, vol 5, pp 2140–2145
4. Zhang N, Kirpitchenko I (2002) Modelling dynamics of a continuous structure with a piezoelectric sensor/actuator for passive structural control. J Sound Vib 249:251–261
5. Miara B, Stavroulakis G, Valente V (eds) (2007) Topics on mathematics for smart systems. Proceedings of the European conference, Rome, Italy, 26–28 October 2006, World Scientific, Singapore
6. Shahian B, Hassul M (1994) Control system design using MATLAB. Prentice-Hall, New Jersey
7. Huang WS, Park HC (1993) Finite element modelling of piezoelectric sensors and actuators. AIAA J 31:930–937

8. Foutsitzi G, Marinova D, Hadjigeorgiou E, Stavroulakis G (2002) Finite element modelling of optimally controlled smart beams. 28th summer school: applications of mathematics in engineering and economics, Sozopol, Bulgaria
9. Stavroulakis GE, Foutsitzi G, Hadjigeorgiou E, Marinova D, Baniotopoulos CC (2005) Design and robust optimal control of smart beams with application on vibrations suppression. Adv Eng Software 36(11–12):806–813
10. Burke JV, Henrion D, Lewis ML (2006) Overton.HIFOO – a MATLAB package for fixed-order controller design and Hinf. optimization. Proceedings of the IFAC symposium on robust control design. Toulouse, France. www.cs.nyu.edu/overton/software/hifoo
11. Tiersten HF (1969) Linear piezoelectric plate vibrations. Plenum Press, New York
12. Burke JV, Henron D, Kewis AS, Overton ML (2006) Stabilization via nonsmooth, nonconvex optimization. Automatic Control IEEE 5(11):1760–1769
13. Bosgra OH, Kwakernaak H (2001) Design methods for control systems. Lecture Notes for a course, Dutch Institute for Systems and Control, The Netherlands, p 69
14. Hou M, Muller PC (1992) Design of observers for linear systems with unknown inputs. IEEE Trans Automat Contr 37:871–875
15. Packard A, Doyle J, Balas G (1993) Linear, multivariable robust control with a μ perspective. ASME J Dyn Syst Meas Contr, 50th Anniversary Issue 115(2b):310–319
16. Pouliezos A (2008) MIMO control systems. Lecture Notes for a course, http://pouliezos.dpem.tuc.gr
17. Marinova D, Stavroulakis GE, Foutsitzi D, Hadjigeorgiou E, Zacharenakis EC (2004) Robust design of smart structures taking into account structural defects. Summer school conference advanced problems in mechanics In: Indeitsev DA (ed) Russian academy of sciences, pp 288–292
18. Tits AL, Yang Y (1996) Globally convergent algorithms for robust pole assignment by state feedback. IEEE Trans Automat Contr 41:1432–1452
19. Ward RC (1981) Balancing the generalized eigenvalue problem. SIAM J Sci Stat Comput 2:141–152
20. Young P, Newlin M, Doyle J (1992) Practical computation of the mixed problem. Proceedings of the American control conference, pp 2190–2194
21. Arvanitis KG, Zacharenakis EC, Soldatos AG, Stavroulakis GE (2003) New trends in optimal structural control. In: Belyaev A, Guran A (ed) Selected topics in structronic and mechatronic system, Chapter 8, World Scientific, Singapore, pp 321–415

View publication stats